Ortho-Substituted Benzofused Macrocyclic Lactams as Zinc Metalloprotease Inhibitors

Gary M. Ksander,* Reynalda de Jesus, Andrew Yuan, R. D. Ghai, A. Trapani, Colin McMartin,† and Regine Bohacek‡

Research Department, Novartis Pharmaceuticals Corporation, 556 Morris Avenue, Summit, New Jersey 07901

Received August 8, 1996⊗

The design and preparation of ortho-substituted benzofused macrocyclic lactams are described. The benzofused macrocyclic lactams were designed as neutral endopeptidase 24.11 (NEP) inhibitors. Docking studies were carried out in a model of thermolysin (TLN) using the MACROMODEL and QXP modeling programs to select suitable ring sizes. These studies predicted that the 11-, 12-, and 13-membered ring macrocyclic lactams would be active in both enzymes TLN and NEP. Good predictability of experimental results, within this series, of binding to thermolysin and to a lesser extent to NEP was observed. A visual comparison, docked at the active site of TLN, is presented for thiorphan, a 10-membered ring macrocycle and an 11-membered ring benzofused macrocyclic lactam. Potent inhibition of both NEP and thermolysin was obtained. The 11-membered ring macrocycle **25a** is the most potent inhibitor from this series of compounds (TLN $IC_{50} = 68$ nM; NEP $IC_{50} = 0.9$ nM). The effects of prodrug **44b** administered at 10 mg/kg po on plasma atrial natriuretic peptide (ANP) levels in conscious rats was greater than 200% over a 4 h period.

Atrial natriuretic peptide (ANP)[1a,b] is a potent diuretic, natriuretic, and vasorelaxant hormone. These properties have led many investigators to speculate that this peptide might be effective for treating hypertension, congestive heart failure, and renal diseases.[2] Numerous groups have independently demonstrated that kidney membrane preparations degrade ANP enzymatically. Furthermore inactivation and the loss of biological activity *in vivo*,[3a−h] at least in part, occurs via cleavage of the Cys[7]−Phe[8] peptide bond, Figure 1, by neutral endopeptidase 24.11[4] (NEP, EC 3.4.24.11). NEP inhibitors have been shown to elicit ANP-like responses in animal models.[5a−g]

To date, selective NEP inhibitors have not fulfilled their potential as therapeutic agents. However, understanding the structural requirements to inhibit this enzyme is still a very intriguing subject. With the understanding of NEP, insights into the inhibitory nature of other structurally similar metalloproteases may be possible. For example, the accompanying paper describes simple modifications to the compounds presented in this paper that converts selective NEP inhibitors into dual ACE/NEP inhibitors.

A potent 10-membered macrocycle NEP inhibitor has previously been described.[6] Our goal was to synthesize benzofused macrocycles and examine the *in vitro* effects of placing a phenyl ring in the S_1' or S_2' subsite of NEP and thermolysin (TLN). In order to select the suitable size of the macrocycle and position for the phenyl ring, we carried out docking studies using the MACROMODEL modeling program based on the crystal structure of TLN. These studies predicted that the 11-, 12-, and 13-membered macrocycles would be active.

The modeling studies have recently been extended using newer, significantly faster methods (QXP) allowing the inclusion of a larger number of compounds and more comprehensive conformational searching. The results of these more recent studies will be described in this publication.

Model for NEP

The three-dimensional structure of NEP has not as yet been reported. However, a related zinc metalloprotease, thermolysin, for which a number of high-resolution crystal structures are readily available,[8] has been used successfully as a model for NEP in the design of NEP inhibitors. Recent examples include a 10-membered macrocyclic thiol[6] and candoxatrilat.[9]

There are significant similarities between the substrate specificity and the inhibitors of NEP and thermolysin. Both enzymes catalyze the hydrolysis of an amide bond on the amino side of hydrophobic residues. Many inhibitors of thermolysin also inhibit NEP. One of the striking similarities of the two enzymes is the stereochemical requirements of the P_1' residue. Unlike ACE, both NEP and thermolysin are inhibited by (*S*)- and (*R*)-thiorphan and (*R*)-retrothiorphan and, to a lesser degree, by (S)-retrothiorphan.[10,11] This indicates that the volume around the base of the S_1' subsite must be similar in both enzymes. The position of the enzyme atoms which form hydrogen bonds to the amide group linking P_1' to P_2' are also likely to be very similar in the two enzymes as inferred from the ability of thiorphan, retrothiorphan, and 10-membered ring lactams to inhibit both NEP and thermolysin.

Relevant to this work is the orientations of the S_1' and S_2' subsites of NEP and thermolysin. In thermolysin these pockets are connected. The crystal structures of several 10-membered macrocycles complexed to thermolysin have been determined and show that these molecules bind to the S_1' and S_2' subsites of thermolysin.[12] Since these 10-membered macrocycles are very potent NEP inhibitors,[6] it can be hypothesized that they also bind to the S_1' and S_2' pockets of NEP and that, as in thermolysin, these subsites form one contiguous accessible volume.

* Author to whom correspondence should be addressed.
† Current address: Thistlesoft, Lindsley Dr., Suite 302, Morris Township, NJ 07960.
‡ Current address: Ariad Pharmaceuticals, Inc., 26 Landsdowne St., Cambridge, MA 02139.
⊗ Abstract published in *Advance ACS Abstracts,* January 15, 1997.

S0022-2623(96)00582-1 CCC: $14.00

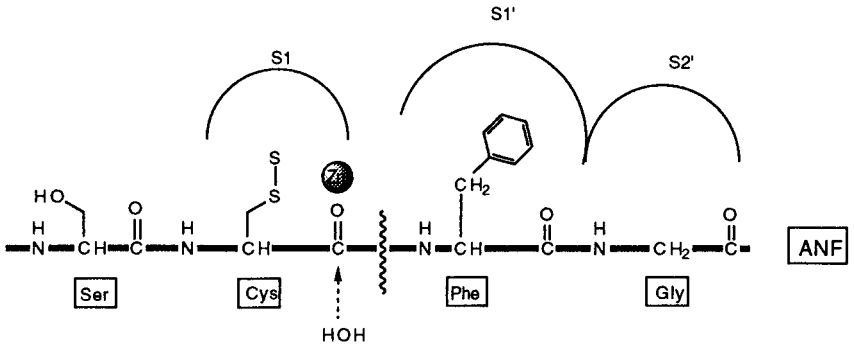

Figure 1. Cleavage site of ANP by NEP 24.11.

A significant difference between thermolysin and NEP is the size of the S_1' pocket. NEP accepts inhibitors with a large group such as a biphenylylmethyl in P_1'[13] whereas such compounds do not inhibit thermolysin. Therefore, when using thermolysin as a model for NEP, it is important to know which regions can be inferred to be structurally similar to NEP and which appear to be significantly different.

To evaluate the potential binding of the benzofused macrocycles to thermolysin/NEP, each macrocycle was docked into the thermolysin active site using the MCDOCK module of the QXP molecular modeling program.[14] This program uses a Monte Carlo searching algorithm and a rapid energy minimization procedure to explore different conformations and binding. The output of this program is an ensemble of low-energy conformations. For each conformation a total energy is reported as well as the ligand strain energy. The total energy (described in the Experimental Section) is useful as a qualitative parameter which, although it cannot predict binding affinities, does differentiate between those inhibitors that can form good interactions with an enzyme binding site and those that cannot. The strain energy is the difference in energy between the bound conformation of the ligand and the lowest energy conformation found after an exhaustive conformational search performed in the absence of the binding site. A ligand strain energy above 25 kJ is taken to be excessively high, indicating that the bound conformation is not energetically accessible to that molecule.

The final evaluation of a docked structure is visual. After conformational searching and energy minimization in the binding site, the structures are inspected to determine if they can form the hydrogen bonds and hydrophobic interactions found in the crystal structure of other thermolysin/inhibitor complexes.[8]

Chemistry

The preparation of P_1' benzofused macrocycles is shown in Scheme 1. *N*-Boc-L-aspartic diethyl ester was reduced with sodium borohydride. The crude diol **1** was stirred at room temperature with dimethoxypropane and *p*-toluenesulfonic acid overnight to give the protected *N*-Boc alcohol **2**. The experimental conditions in the acetonide formation for compound **2** theoretically could give two products, a 5- or 6-membered ring. Verification of the structure was accomplished after conversion to the aldehyde. Oxidation with PCC gave the aldehyde **3a**. The proton NMR was consistent with the assigned structure of the 5-membered ring based on the coupling of the aldehyde proton to the two adjacent methylene protons. The aldehyde proton appears at 9.77 ppm as a triplet, $J = 1.8$ Hz. Wittig condensation of the ylide, generated from the phosphonium salt **11** and potassium *tert*-butoxide, with aldehyde **3a** gave a good yield of olefin **12**. Compound **11** was prepared from *o*-bromobenzaldehyde from a series of standard organic transformations. Halogen lithium exchange with nBuLi followed by condensation of the resulting anion with DMF gave the aromatic aldehyde **13**. Condensation of methyl benzyl malonate with aldehyde **13** followed by hydrogenation gave the mono acid ester **15**. Acid hydrolysis of the Boc acetonide with HCl gave the amino alcohol acid ester **16** isolated as a crude reaction mixture. The macrolactonization was accomplished by stirring, under high dilution, the amino acid **16** with EDCI, hydroxybenzhydrazole and triethylamine in methylene chloride. The lactam **17** was oxidized with sodium periodate and ruthenium trichloride, saponified to the diacid with NaOH, and converted to the exocyclic enone **20** with paraformaldehyde–piperidine. Addition of thioacetic acid and reesterification with diazomethane or cesium carbonate/methyl iodide followed by flash chromatography gave two diastereomers **22a** and **22b**. The individual diastereomers **22a,b** were hydrolyzed with LiOH to give the (*S,S*)-**23a** and (*R,S*)-**23b** thiol acids. The *S*-acetyl benzyl esters **44a,b** were prepared similarly by reacting the *S*-acetyl acids **21** with cesium carbonate and benzyl bromide.

The stereochemical assignment of the *S*-acetyl methyl esters is based upon the corresponding chemical shifts determined for the 10-membered ring macrocycle,[6] the cysteine-containing macrocycle,[7] and the meta-substituted benzofused macrocycles described in the following paper. The assignment is also supported by the X-ray of the 10-membered ring macrocycle[6] and the X-ray of the (*R,S*)-meta-substituted benzofused macrocycle described in the following paper.

The ^{1}H NMR chemical shifts of the *S*-acetyl methyl esters NCHCO methine proton appear at 3.9, 4.08, and 4.40 ppm for the (*S,S*) isomers of the 11-, 12-, and 13-membered rings, respectively, to the NCHCO methine protons of the (*R,S*) isomers which appear downfield to the corresponding (*S,S*) diastereomers. The 11-, 12-, and 13-membered ring (*R,S*) NCHCO methine protons appear at 4.50, 4.65, and 4.63 ppm, respectively.

The general procedure, described above, was used to prepare the 11-(**25a,b**) and 13-(**27a,b**) membered ring macrocycles. The ring size of the macrocycle was controlled by adjusting the chain length of the aryl phosphonium salt and/or the aldehyde **3a,b** derived from either L-aspartic acid or L-glutamic acid. The 11-membered ring was prepared from the ylide derived from 2-bromobenzyl bromide and the aldehyde derived from L-glutamic acid. The 13-membered ring was

Scheme 1[a]

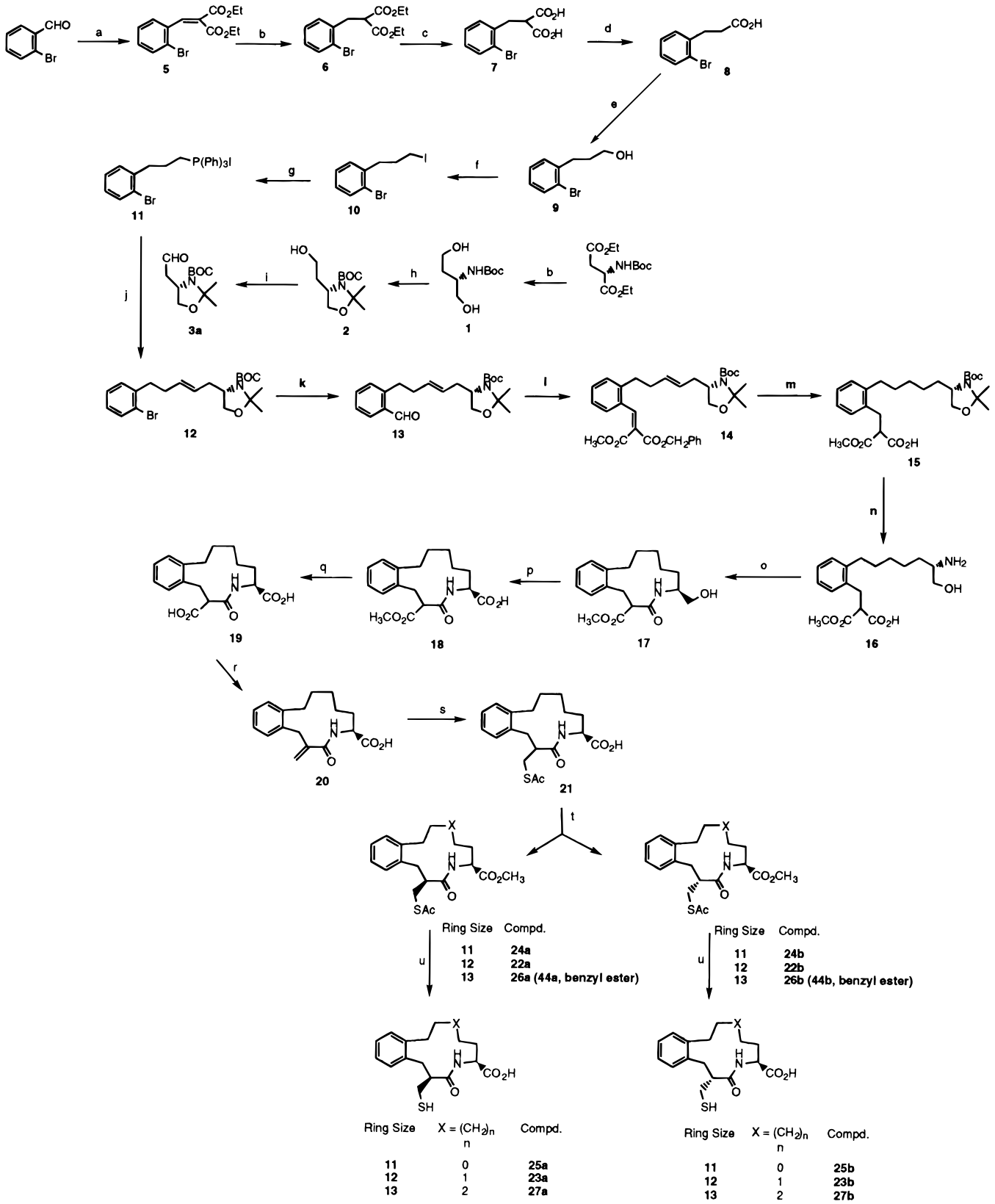

[a] Reagents: (a) diethyl malonate, piperidine; (b) $NaBH_4$; (c) KOH; (d) 180 °C; (e) 1 M borane−THF complex,; (f) triphenylphosphine, *N*-iodosuccinimide; (g) triphenylphosphine; (h) dimethoxypropane, pTSA; (i) pyridinium chlorochromate; (j) *t*-BuOK; (k) BuLi, DMF; (l) benzyl methyl malonate, piperidine, benzoic acid; (m) H_2/Pd−C; (n) HCl; (o) EDCI, HOBT; (p) $NaIO_4$, $RuCl_3$; (q) NaOH; (r) paraformaldehyde, piperdine; (s) thiolacetic acid; (t) cesium carbonate, methyl iodide; (u) LiOH.

prepared from the ylide derived from 1-iodo-3-(2-bromophenyl)propane and the aldehyde derived from L-glutamic acid.

The preparation of P_2' benzofused macrocycles is shown in Scheme 2. *d,l-o*-Bromo-*N*-BOC-phenylalanine ethyl ester was reduced with sodium borohydride to the alcohol followed by stirring at room temperature with dimethoxypropane and *p*-toluenesulfonic acid overnight to give the racemic protected *N*-Boc derivative **28.** The aromatic bromide was lithiated with nBuLi and reacted

Scheme 2[a]

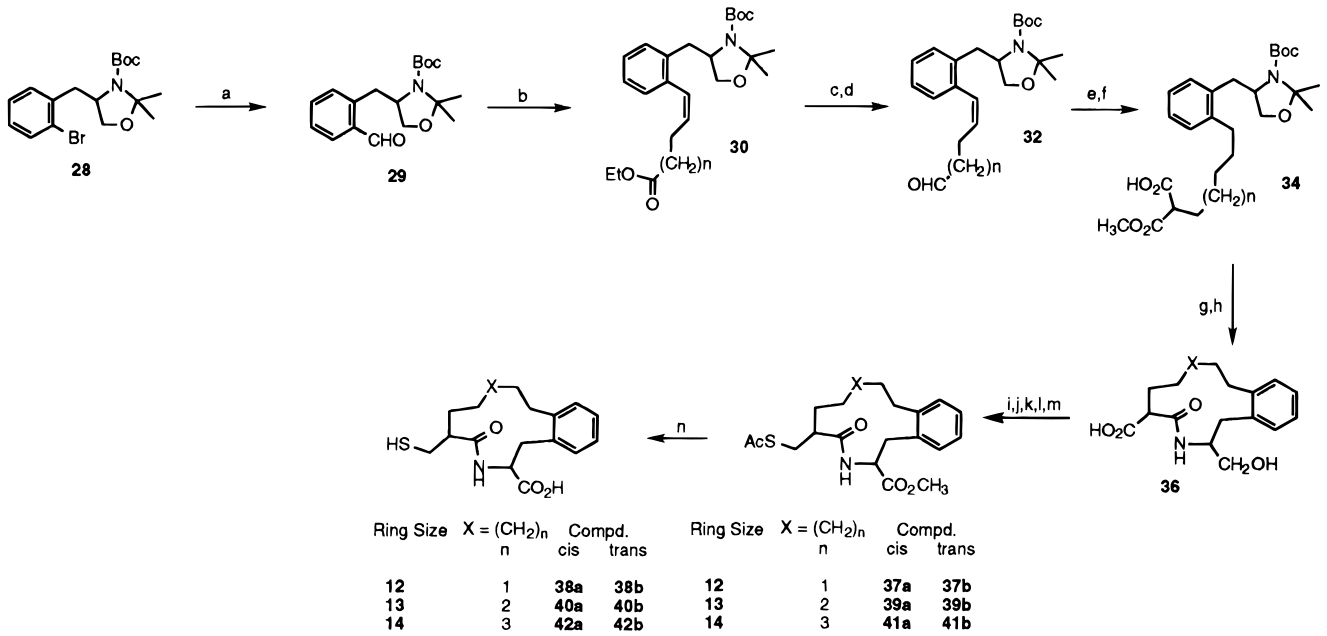

Ring Size	X = $(CH_2)_n$ n	Compd. cis	Compd. trans	Ring Size	X = $(CH_2)_n$ n	Compd. cis	Compd. trans
12	1	**38a**	**38b**	12	1	**37a**	**37b**
13	2	**40a**	**40b**	13	2	**39a**	**39b**
14	3	**42a**	**42b**	14	3	**41a**	**41b**

[a] Reagents: (a) BuLi, DMF; (b)$Ph_3I(CH_2)_xCO_2Et$, KOtBu; (c) lithium aluminum hydride; (d) pyridinium chlorochromate; (e) benzyl methyl malonate, piperidine, benzoic acid; (f) H_2/Pd−C; (g) HCl; (h) EDCI, HOBT; (i) $NaIO_4$, $RuCl_3$; (j) NaOH; (k) paraformaldehyde, piperdine; (l) thiolacetic acid; (m) cesium carbonate, methyl iodide; (n) LiOH.

with DMF. The resulting aldehyde **29** was condensed with the appropriate ylide using standard Wittig conditions. The phosphonium salts derived from ethyl 4-iodobutyrate, ethyl 5-iodovalerate, and ethyl 6-iodohexanoate led to the preparation of the 12-, 13-, and 14-membered ring macrocycles, respectively.

The ester **30** was reduced with lithium aluminum hydride and reoxidized to the aldehyde **32**. Base-catalyzed condensation of aldehyde **32** with the mixed benzyl ethyl malonate followed by palladium catalyzed hydrogenation gave the mixed acid ethyl ester **34**. Acid hydrolysis and EDCI/HOBT cyclization under dilute reaction conditions gave the macrocyclic lactam **36**.

The lactam **36** was converted to the thiol acids **38**, **40**, and **42** as outlined in the previous examples described for the P_1' benzofused macrocycles. The starting material *o*-bromophenylalanine was racemic; therefore the P_2' benzofused lactams were isolated as the racemic cis and racemic trans products. However, in the preparation of the 12-membered ring macrocycle only one *S*-acetyl methyl ester isomer **37** was isolated. On the basis of the chemical shift of the NCHCO methine proton, 5.18 ppm, a tentative trans stereochemical assignment has been made.

Results and Discussion

We demonstrate that the relative ability of benzofused macrocycles to bind to TLN and to a lesser extent NEP can be predicted on the basis of the proposed molecular model. The benzofused macrocycles can be considered hybrids of thiorphan, Figure 2, and the 10-membered ring macrocycle **43**, Figure 3. Essential to the binding of these compounds to TLN is proper orientation of the thiol and the amide bond. Both compounds thiorphan and **43** can easily adopt the required conformation, consistent with the model. However neither of these two compounds effectively fill the S_1' and S_2' binding sites of thermolysin. The P_1' benzofused macrocycles have been designed to position the phenyl ring into the S_1' subsites in a manner similar to that for thiorphan.

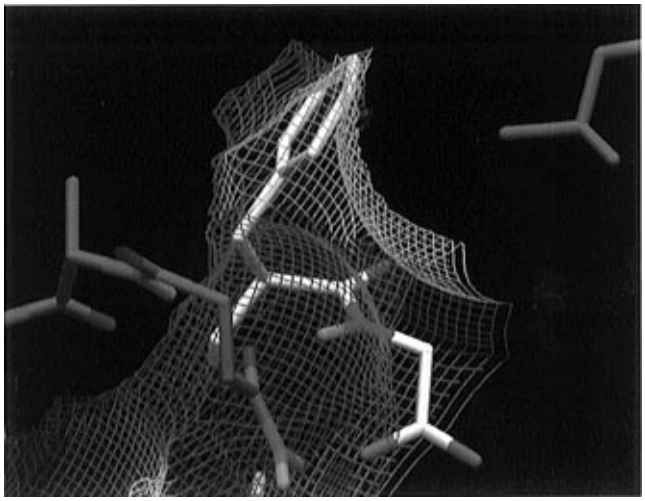

Figure 2. Thiorphan (IC_{50} = 9500 nM TLN and 4.3 nM NEP) in the active site of thermolysin.

In addition, the alkane chain connecting the phenyl ring to the terminal carboxylic acid was designed to extend along the hydrophobic region between the S_1' and S_2' subsites similar to the aliphatic macrocycles previously reported.[6,7] Molecular modeling was used to determine which size macrocycle would be ideal to achieve these goals. Macrocycles ranging in size from 10 to 14 were modeled. The 10-membered ring was too small and the 14-membered ring too large. However, low-energy conformation of the 11-, 12-, and 13-membered rings reveal an excellent fit of the aromatic ring into the P_1' pocket as well as good hydrophobic interaction between the alkane chain and the $S_1'-S_2'$ sites of thermolysin. On the basis of these findings, the 11-, 12-, and 13-membered macrocycles were synthesized. The NEP and thermolysin *in vitro* data is shown in Table 1.

As previously mentioned, the benzofused macrocycles, Table 1, were designed as hybrids of thiorphan and the 10-membered ring macrocycle **43**. Thiorphan and **43**, bound to the active site of thermolysin, are shown in Figures 2 and 3,[22] respectively. In Figure 2, the phenyl

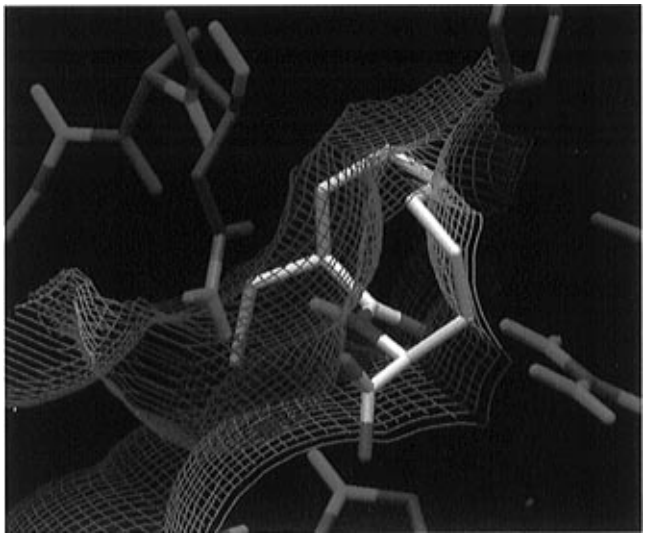

Figure 3. Ten-membered ring macrocycle **43** (IC_{50} = 8800 nM TLN and 17 nM NEP) in the active site of thermolysin.

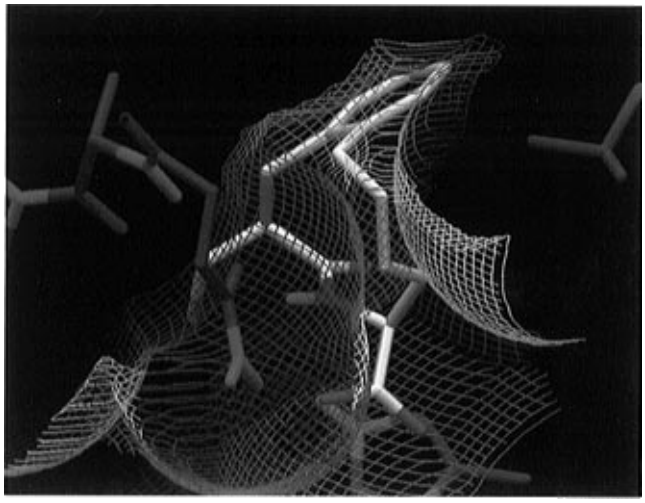

Figure 4. Compound **25a** (IC_{50} = 68 nM TLN and 0.9 nM NEP) in the active site of thermolysin.

Table 1. *In vitro* NEP, ACE, and Thermolysin Inhibition of P_1' Ortho-Substituted Benzofused Macrocyclic Lactams

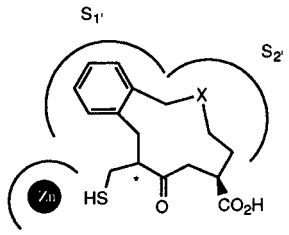

compd	ring size X = $(CH_2)_n$	stereochem	IC_{50} (nM) NEP	IC_{50} (nM) TL	molecular model total energy (kJ/mol)	molecular model ligand strain energy (kJ/mol)
25a	11	S	0.9	68	−31.2	3
25b	11	*R*	7	2300	−26.4	6
23a	12	S	3	600	−29.4	8
23b	12	*R*	4	4000	−19.7	13
27a	13	S	224	41000	−27.8	12
27b	13	*R*	27	1800	−29.9	9

ring of thiorphan extends slightly beyond the accessible surface of the model. This may explain the moderate binding of thiorphan to thermolysin (IC_{50} = 9500 nM). Binding to NEP, IC_{50} = 4.3 nM, should not be affected since the P_1' pocket is deep enough to accommodate a biphenyl group. The 10-membered ring macrocycle, **43**, lacking good occupation of the P_1' pocket, relies upon the hydrophobic interactions of the methylene chain for additional binding affinity. The 10-membered macrocycle, **43**, readily fits into the contiguous volume between the S_1' and S_2' sites of thermolysin. However, this compound does not fully occupy the S_1' subsite. This may cause the relatively weak binding of this compound (IC_{50} = 9500 nM) to thermolysin.

Macrocycle **25a** is the most potent thermolysin inhibitor (IC_{50} = 68 nM) from this series of compounds. It is also the most potent inhibitor of NEP, IC_{50} = 0.9 nM. Figure 4 shows compound **25a** bound to the active site of TLN. In contrast to thiorphan, the phenyl ring of **25a** makes excellent hydrophobic contacts with the accessible surface of the S_1' pocket. Figure 4 also shows good hydrophobic interactions of the methylene tether along the S_1' and the S_2' sites of the enzyme. In addition to hydrophobic interactions, another very important parameter to good binding is the ability to form acceptable hydrogen bonds. In the model, the distance between the carbonyl oxygen and the hydrogens of Arg 203 were 2.3 and 2.4 Å for the 11-membered (*S*,*S*) isomer **25a** and 2.8 and 2.8 Å for the (*R*,*S*) isomer **25b**. This is reflected in the total energy. In agreement with these findings, the total energy computed for **25a** was the lowest of all the macrocycles.

Although the total energy cannot be used to rank order the potency of the entire series, we examined the ability of the model to predict potency of each pair of stereoisomers. For the 11-membered macrocycles, the modeling studies indicate that the cis (*S*,*S*) isomer, **25a**,

Table 2. *In vitro* NEP, ACE, and Thermolysin Inhibition of P_2' Ortho-Substituted Benzofused Macrocyclic Lactams

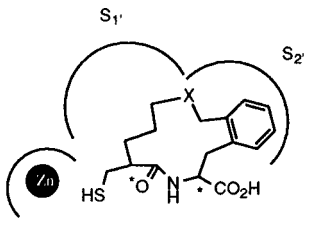

compd	ring size X = $(CH_2)_n$	stereochem	IC_{50} (nM) NEP	IC_{50} (nM) TL	molecular model total energy (kJ/mol)	molecular model ligand strain energy (kJ/mol)
38b	12	*RS*,*SR* (trans)	99	49000		
40a	13	*SS*,*RR* (cis)	67	40000	(*S*,*S*) −27.2	(*S*,*S*) 16
40b	13	*RS*,*SR* (trans)	136	16000	(*R*,*S*) −14.0	(*R*,*S*) 8
42a	14	*SS*,*RR* (cis)	900	NT	(*S*,*S*) −24.2	(*S*,*S*) 13
42b	14	*RS*,*SR* (trans)	>10000	60000		

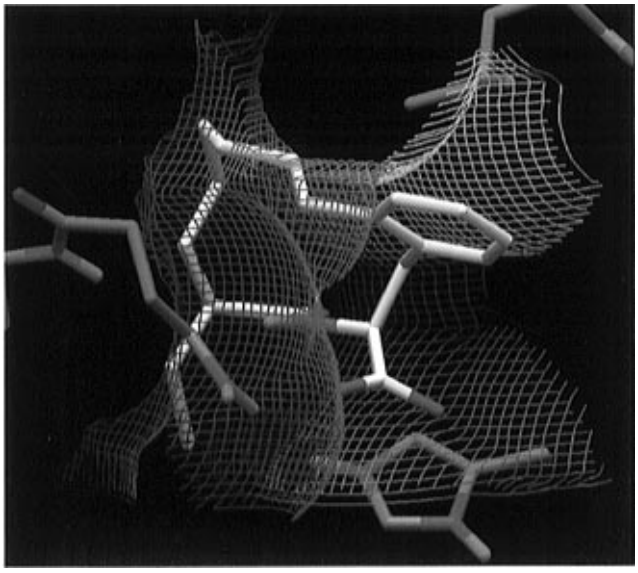

Figure 5. Compound **40a** (racemic cis IC_{50} = 40 000 nM TLN and 67 nM NEP) in the active site of thermolysin.

should be more potent than the trans (*R,S*)-**25b** isomer. This is consistent with experimental results (Table 1). Similarly, the (*S,S*) cis 12-membered ring diastereomer **23a** is more potent in TLN than the corresponding trans isomer **23b**. Interestingly, for the 13-membered ring isomers, the (*R,S*) trans isomer **27b** fits the model more effectively than the (*S,S*) cis isomer **27a**. This reversal of the predicted stereochemistry preference, cis to trans, is also consistent with experimental results.

In our model, the P_2' benzofused macrocycles position an aromatic ring into the S_2' subsite of thermolysin. A portion of the aromatic ring is in a hydrophobic region, flanked by Phe 130, Leu 202, and Tyr 193. However, a substantial portion of the aromatic ring protrudes into the solvent, Figure 5. Although these macrocycles occupy more of the $S_1'-S_2'$ subsite than the unsubstituted 10-membered macrocycle, they do not fill the S_1' subsite of thermolysin nearly as well as the P_1' series of benzofused macrocycles.

Upon synthesis, it was found that the P_2' benzofused macrocycles are considerably poorer inhibitors of both thermolysin and NEP. Therefore, we conclude that full occupation of the solvent inaccessible S_1' subsite greatly enhances binding whereas occupation of the more solvent accessible S_2' subsite is unfavorable.

ANP Potentiation Assay

Although the emphasis of this paper deals with the rationalization of the *in vitro* activity of this series of compounds, we present some *in vivo* activity to demonstrate oral activity in a functional animal model of ANP.

Plasma ANP concentrations were determined in animals infused with exogenous ANP before and after administration of NEP inhibitors. Figure 6 shows the effects of **44b** administered at 10 mg/kg po on plasma ANP levels in conscious rats. Plasma ANP levels are expressed as a percent of those measured in vehicle-treated animals which received the infusion of exogenous ANP. ANP levels were increased significantly, greater than 200%, at all time points (30−240 min) after the administration of **44b.**

In summary, a series of ortho-substituted benzofused macrocyclic lactams were examined in a model of

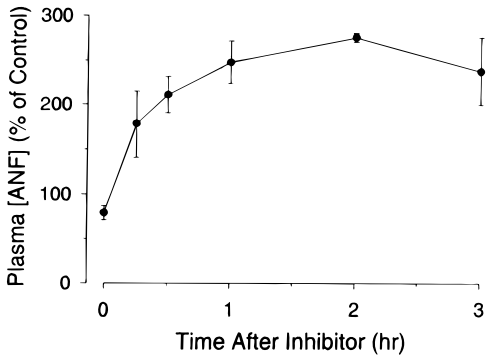

Figure 6. The effect of **44b** administered orally at 10 mg/kg on plasma ANF concentrations in conscious rats infused with exogenous ANF. Values are the mean ± SEM for six rats treated with **44b**.

thermolysin which resulted in good predictability of experimental results, within this series, of binding to thermolysin and to a lesser extent to NEP. Potent inhibition of both NEP and thermolysin was obtained. To demonstrate *in vivo* efficacy within this series of compounds, a prodrug of **26b** was prepared which produced marked increases of ANP levels upon oral administration at 10 mg/kg in rats.

Experimental Section

General Procedures. ^{1}H NMR spectra were recorded on Varian XL 400 MHz, Varian VR 300 MHz, and/or Bruker AC 250 MHz spectrometers with tetramethylsilane as internal standard. Infrared spectra were recorded on a Nicolet 5SXFT spectrometer. Optical rotations were measured with a Perkin-Elmer Model 241 polarimeter. Melting points were taken on a Thomas-Hoover melting point apparatus and are uncorrected.

2(*S*)-[[(1,1-Dimethylethoxy)carbonyl]amino]-1,4-butanediol (1). To a solution of *N*-Boc diethyl L-aspartic acid ester (22.9 g, 79.4 mmol) in 300 mL of ethanol cooled in an ice bath was added sodium borohydride (24 g, 8 eqv). The reaction was refluxed for 4 h, cooled, poured into brine, and extracted with ether. The organic layer was dried ($MgSO_4$), filtered, and evaporated to dryness to give 15.8 g (97%) of **1**: ^{1}H NMR ($CDCl_3$) δ 5.0 (d,1H), 3.83 (m, 1H), 3.7 (m, 4H), 1.8 (m, 1H), 1.6 (m, 1H), 1.4 (s, 9H).

2,2-Dimethyl-3-[(1,1-dimethylethoxy)carbonyl]-4(*S*)-oxazolidineethanol (2). The diol **1** (15.8 g, 77 mmol) in 350 mL of methylene chloride, dimethoxypropane (96 mL), and *p*-toluenesulfonic acid (1.5 g, 7.7 mmol) were stirred at room temperature for 16 h. The organic layer was washed with $NaHCO_3$ (2×) and brine, dried ($MgSO_4$), evaporated to dryness, and flash chromatographed on silica gel eluting with ethyl acetate/hexane (1:2) to give 8.0 g (42%) of **2**: ^{1}H NMR ($CDCl_3$) δ 4.2 (m, 1H), 4.0 (m, 2H), 3.68 (d, 1H), 3.6 (m, 1H), 1.8 (m, 2H), 1.65 and 1.55 (s, 3H), 1.47 (s, 9H).

2,2-Dimethyl-3-[(1,1-dimethylethoxy)carbonyl]-4(*S*)-oxazolidineacetaldehyde (3a). The solution of alcohol **2** (7.98 g, 32 mmol) and pyridinium chlorochromate (14 g, 65 mmol) in 120 mL of methylene chloride was stirred for 2.5 h, diluted with ether, and stirred for an additional 5 min. The residue was removed by filtering the suspension through a small plug of silica gel. The organic solute was concentrated to dryness and flash chromatographed on silica gel, eluting with ethyl acetate/hexane (1:4) to give 5.6 g (74%) of **3a**: ^{1}H NMR ($CDCl_3$) δ 9.77 (t, J = 1.8 Hz, 1H), 4.3 (m, 1H), 4.07 (m, 1H), 3.7 (d, 1H), 3.1−2.5 (m, 2H), 1.6 (s, 3H), 1.52 (s, 3H), 1.45 (s, 9H).

2,2-Dimethyl-3-[(1,1-dimethylethoxy)carbonyl]-4(*S*)-oxazolidinepropanal (3b): ^{1}H NMR ($CDCl_3$) δ 9.75 (s, 1H), 3.95 (m, 2H), 3.2 (d, 1H), 2.47 (t, 2H), 1.96 (m, 2H), 1.1 (s, 3H), 1.52 (s, 3H), 1.42 (s, 9H).

Diethyl [(2-Bromophenyl)methylene]propanedioate (5). To a solution of 2-bromobenzaldehyde (37 g, 0.2 mol), diethyl malonate (32 g, 0.2 mol), and piperidine (2.56 g, 0.03

mol) was added benzoic acid (2.46 g, 0.02 mol) in 120 mL of toluene. The reaction mixture was refluxed with water removal using a Dean−Stark condenser for 3 h. The mixture was cooled to room temperature and diluted with ether (400 mL) and ethyl acetate (100 mL), and the organic layer was washed with 2 N HCl (2×), $NaHCO_3$ (2×), and brine, dried ($MgSO_4$), and evaporated to dryness to give 65.2 g (100%) of **5** as a brown oil: ^{1}H NMR ($CDCl_3$) δ 7.95 (s, 1H), 7.6 (d, 1H), 7.4 (d, 1H), 7.25 (m, 2H), 4.31 (q, 2H), 4.2 (q, 2H), 1.33 (t, 3H), 1.17 (t, 3H).

Diethyl [(2-Bromophenyl)methyl]propanedioate (6). Sodium borohydride (2 g) was added to an ice bath cooled solution of **5** (65.2 g, 0.2 mol) in 150 mL of ethanol. The solution was stirred for 30 min. A second portion of sodium borohydride (2 g) was added, and the reaction mixture was stirred for 30 min followed by a third addition of sodium borohydride (2 g). Glacial acetic acid was added cautiously, the mixture was concentrated, and the reside was taken up in ether and washed with 1 N HCl, 3 × $NaHCO_3$, and brine, dried over $MgSO_4$, filtered, and evaporated to dryness to give 58 g (89%) of **6**: ^{1}H NMR ($CDCl_3$) δ 7.54 (d, 1H), 7.2 (m, 2H), 7.05 (m, 1H), 4.15 (q, 4H), 3.83 (t, 1H), 3.3 (d, 2H), 1.2 (q, 6H).

[(2-Bromophenyl)methyl]propanedicarboxylic Acid (7). To a solution of potassium hydroxide (27.1 g 0.42 mol) in 90 mL of water was added the diester **6** (58.1 g, 0.176 mol). The mixture was refluxed for 7 h and stirred at room temperature overnight. The aqueous reaction mixture was washed with ether, cooled in an ice bath, and acidified with concentrated HCl to pH 2. The solid was collected, washed with water, and dried at 50 °C under high vacuum to give 36.1 g (75%) of **7** as a solid: ^{1}H NMR ($CDCl_3$), δ 7.65 (d, 1H), 7.3 (d, 2H), 7.05 (m, 1H), 3.68 (t, 2H), 3.15 (d, 2H).

2-Bromobenzenepropanoic Acid (8). The dicarboxylic acid **7** (36 g, 0.131 mol) was heated at 180 °C for 5 h. To the hot mixture was added 50 mL of water, and the mixture was cooled and then acidified with 50 mL of 1 N HCl. The aqueous solution was decanted from the product. The solid was dissolved in methylene chloride washed with water, treated with activated charcoal, dried over $MgSO_4$, filtered, and evaporated to dryness to give 24.4 g (81%) of **8** as a soft brown solid: ^{1}H NMR ($CDCl_3$) δ 7.52 (d, 1H), 7.2 (m, 2H), 7.05 (m, 1H), 3.04 (t, 2H), 2.7 (t, 2H).

2-Bromobenzenepropanol (9). To a solution of acid **8** (24.4 g, 0.101 mol) in 80 mL of THF cooled in an ice bath was added 1.0 M borane in THF (426 mL, 43 mmol) over a 30 min period. After the addition was complete the mixture was refluxed for 30 min. To the cooled mixture was added slowly 6 N HCl (120 mL), and the solution was heated to 60 °C for 30 min and then stirred at room temperature overnight. The reaction mixture was concentrated followed by the addition of 70 mL of water and 200 mL of ether. The organic layer was washed (2×) with water, dried over $MgSO_4$, filtered, and evaporated to dryness to give 23 g of **9** (96%) as a colorless oil: ^{1}H NMR ($CDCl_3$) δ 7.52 (d, 1H), 7.2 (m, 2H), 7.05 (m, 1H), 3.7 (t, 2H), 2.84 (t, 2H), 1.9 (m, 2H).

1-Bromo-2-(3-iodopropyl)benzene (10). To a solution of aryl alcohol **9** (17.5 g, 81.6 mmol) in 250 mL of methylene chloride, cooled in an ice bath, was added triphenylphospine (25.7 g, 98 mmol) followed by dropwise addition of *N*-iodosuccinamide (20.2 g, 90 mmol). The reaction mixture was stirred at room temperature overnight, 15 g of silica gel was added, and the solvent was removed at the rotory evaporator. Hexanes (50 mL) were added, and the suspension was added to a column of silica gel and chromatographed eluting with hexane/methylene chloride (95:5) to give 7.54 g (29%) of **10** as an oil: ^{1}H NMR ($CDCl_3$) δ 7.5 (d, 1H), 7.2 (m, 2H), 7.08 (m, 1H), 3.18 (t, 2H), 2.8 (t, 2H), 2.1 (m, 2H).

[3-(2-Bromophenyl)propyl]iodotriphenylphosphorane (11). A mixture of aryl iodide **10** (12.3 g, 37.9 mmol) and triphenylphosphine (9.97 g, 38 mmol) in 125 mL of toluene was refluxed for 17 h and cooled, and the solid was collected. The product was washed with ether and dried under high vacuum to give 16 g (70%) of **11** as a colorless solid: ^{1}H NMR ($CDCl_3$) δ 7.7 (m, 15H), 7.52 (d, 1H), 7.41 (d, 1H), 7.20 (d, 1H), 7.0 (t, 1H), 3.77 (m, 2H), 3.15 (t, 2H), 2.0 (m, 2H).

4(*S*)-[5-(2-Bromophenyl)-2-pentenyl]-2,2-dimethyl-3-[(1,1-dimethylethoxy)carbonyl]oxazolidine (12). To a mixture of phosphonium salt **11** (15.6 g, 26.6 mmol) and aldehyde **3a** (4.32 g, 17.8 mmol) in 200 mL of methylene chloride was added 26.6 mmol of 1.6 M potassium *tert*-butoxide in THF at 0 °C. Disappearance of starting material was monitored by TLC (0.5 h). To the reaction mixture was added silica gel, and the mixture was evaporated to dryness and flash chromatographed on silica gel eluting with ether/hexane (1:4) to give 3.79 g (51%) of **12** as a yellow oil: ^{1}H NMR ($CDCl_3$) δ 7.5 (d, 1H), 7.18 (m, 2H), 7.03 (m, 1H), 5.03 (m, 1H), 5.34 (m, 1H), 3.81 and 3.62 (dd, 2H), 3.7 (m, 1H), 2.77 (t, 2H), 2.37 (q, 2H), 2.3 (m, 2H), 1.6 (m, 6H), 1.43 (s, 9H).

2-[5-[2,2-Dimethyl-3-[(1,1-dimethylethoxy)carbonyl]-oxazolidin-4(*S*)-yl]-3-pentenyl]benzaldehyde (13). The aryl bromide **12** (3.65 g, 8.63 mmol) in 100 mL of THF was cooled to −78 °C. A solution of 2.5 N nBuLi (5.52 mL, 13.8 mmol) was added dropwise. After completion of nBuLi addition, DMF was added, and the mixture was warmed to 0 °C over a 1 h period. The reaction solution was poured into ice water and extracted with ether two times. The ethereal layer was washed with water (2×) and brine (2×), dried over $MgSO_4$, filtered, and evaporated to dryness. The residue was flash chromatographed on silica gel, eluting with ether/hexane (1:4), affording 2.28 g (71%) of **13**: ^{1}H NMR ($CDCl_3$) δ 10.2 (d, 1H), 7.8 (d, 1H), 7.5 (t, 1H), 7.3 (m, 2H), 5.54 (m, 1H), 5.32 (m, 1H), 3.7 (m, 2H), 3.6 (d, 1H), 3.1 (t, 2H), 2.4 (q, 2H), 2.2 (m, 2H), 1.6 (s, 3H), 1.55 (s, 3H), 1.50 (s, 9H).

Methyl Phenylmethyl [[2-[5-[2,2-Dimethyl-3-[(1,1-dimethylethoxy)carbonyl]oxazolidin-4(*S*)-yl]-3-pentenyl]-phenyl]methylene]propanedioate (14). A mixture of benzyl methyl malonate (1.41 g, 6.45 mmol), piperidine (82 mg, 0.9 mmol), benzoic acid (78.8 mg, 0.64 mmol), and the aldehyde **13** (2.41 g, 6.45 mmol) in 50 mL of toluene was refluxed with water removal using a Dean−Stark condenser for 6 h. The mixture was cooled to room temperature, stirred overnight, and diluted with ether. The organic layer was washed with 1 N HCl (2×), $NaHCO_3$ (2×), and brine (2×), dried ($MgSO_4$), and evaporated to dryness. The residue was chromatographed on silica gel, eluting with ether/hexane (1:3) to give 2.36 g (66%) of **14** as a mixture of geometric isomers: ^{1}H NMR ($CDCl_3$) δ 8.04 (m, 1H), 7.4−7.0 (m, 9H), 5.4 (m, 1H), 5.3 (m, 1H), 5.3 and 5.1 (s, 2H), 3.8 and 3.7 (s, 3H), 3.75 (m, 3H), 2.7 (m, 2H), 2.3 (m, 3H), 1.5 (s, 6H), 1.46 and 1.41 (two singlets, 9H).

[[2-[5-[2,2-Dimethyl-3-[(1,1-dimethylethoxy)carbonyl]-oxazolidin-4(*S*)-yl]pentyl]phenyl]methyl]propanedioic Acid 1-Methyl Ester (15). A suspension of 10% Pd/C (2.0 g) and diester **14** (2.36 g, 4.27 mmol) in 200 mL of ethyl acetate was hydrogenated at 50 psi for 17 h. The reaction mixture was concentrated and filtered through a pad of Celite. The solvent was removed to give 1.9 g of **15** used as is in the next step; ^{1}H NMR ($CDCl_3$) δ 7.1 (m, 4H), 3.9 (m, 1H), 3.71 (s, 3H) 3.70 (m, 2H), 3.27 (m, 3H), 2.6 (m, 2H), 1.7−1.2 (m, 14H), 1.45 (s, 9H).

[[2-(6(*S*)-Amino-7-hydroxyheptyl)phenyl]methyl]propanedioic Acid 1-Methyl Ester (16). A solution of **15** (2.0 g, 10.2 mmol) in 20 mL of methylene chloride at 0 °C was purged with dry HCl gas for 5 min. The ice bath was removed, HCl gas was bubbled into the solution for an additional 5 min, and the solution was stirred at room temperature overnight. The solvent was removed, and the residue **16** was used as is in the next step.

Methyl 1,2,3,4,5,6,7,8,9,10-Decahydro-5(*S*)-(hydroxymethyl)-3-oxo-4-benzazacyclododecine-2-carboxylate (17). To a solution of EDCI (1.77 g, 9.26 mmol) and hydroxybenzotriazole (0.937 g, 6.9 mmol) in 2 L of methylene chloride was slowly added **16** (1.73 g, 4.63 mmol) in triethylamine (7.4 g, 10.2 mmol) and 300 mL of methylene chloride. The solution was mixed with a mechanical stirrer overnight. The solvent was removed under reduced pressure, and the residue was taken up in ethyl acetate and sodium bicarbonate. The organic layer was separated. The aqueous layer was reextracted with ethyl acetate, and the organics were combined, washed with 1 N HCl, and brine, dried ($MgS0_4$), filtered, and evaporated to dryness. The residue was chromatographed on silica gel, eluting with ethyl acetate to give 322 mg (22%) of **17** as a mixture of diastereomers: ^{1}H NMR ($CDCl_3$) δ 7.14 (m, 4H), 6.5 (d, 1H), 4.65 (m, 1H), 4.3 (m, 2H), 3.75 and 3.66 (s, 3H), 3.25−2.8 (m, 3H), 2.65 (m, 2H), 1.9−1.0 (m, 8H).

1,2,3,4,5,6,7,8,9,10-Decahydro-3-oxo-4-benzazacyclododecine-2,5(*S*)-dicarboxylic Acid 2-Methyl Ester (18). The macrocyclic lactam alcohol **17** (322 mg, 1.0 mmol) in 15 mL of acetonitrile and 15 mL of water was oxidized with sodium periodate (864 mg, 4.0 mmol) and ruthenium trichloride hydrate (5 mg, 0.022 mmol). The mixture was stirred for 15 min at room temperature and left to stand for 2 h. The reaction mixture was diluted with methylene chloride, and the organic layer was washed with water, dried ($MgSO_4$), filtered, and evaporated to dryness to give 280 mg (84%) of **18** as a crude mixture of diastereomers. The compound was used without further purification in the next step.

1,2,3,4,5,6,7,8,9,10-Decahydro-3-oxo-4-benzazacyclododecine-2,5(*S*)-dicarboxylic Acid (19). To a solution of **18** (280 mg, 0.84 mmol) in 2 mL of methanol was added 1 N NaOH (2.1 mL, 2.5 equiv). The reaction mixture was stirred at room temperature for 4 h and acidified with 1 N HCl. The precipitate was collected, washed with water, and dried under high vacuum to give 200 mg (75%) of **19** as a mixture of diastereomers.

1,2,3,4,5,6,7,8,9,10-Decahydro-2-methylene-3-oxo-4-benzazacyclododecine-5(*S*)-carboxylic Acid (20). A mixture of **19** (200 mg, 0.62 mmol), piperidine (10.6 mg, 0.125 mmol), and paraformaldehyde (28.2 mg, 0.94 mmol) in 1 mL of pyridine was heated for 3 h at 60 °C. The reaction mixture was concentrated, taken up in ethyl acetate, washed with 1 N HCl and brine, dried ($MgSO_4$), filtered, and concentrated to give 158 mg (88%) of **20**: ^{1}H NMR ($CDCl_3$) δ 7.14 (m, 4H), 5.8 (d, 1H), 5.79 (s, 1H), 5.6 (s, 1H), 4.6 (m, 1H), 3.84 and 3.52 (dd, 2H), 2.9 (m, 1H), 2.65 (m, 1H), 2.0−1.0 (m, 8H).

2-[(Acetylthio)methyl]-1,2,3,4,5,6,7,8,9,10-decahydro-3-oxo-4-benzazacyclododecine-5(*S*)-carboxylic Acid (21). A mixture of thiol acetic acid (3 mL) and **20** (158 mg, 0.55 mmol) was stirred for 24 h at room temperature. The solution was concentrated to give **21**. The material was used crude in the next reaction.

Methyl 2(*S*)-[(Acetylthio)methyl]-1,2,3,4,5,6,7,8,9,10-decahydro-3-oxo-4-benzazacyclododecine-5(*S*)-carboxylate (22a) and Methyl 2(*R*)-[(Acetylthio)methyl]-1,2,3,4,5,6,7,8,9,10-decahydro-3-oxo-4-benzazacyclododecine-5(*S*)-carboxylate (22b). To a suspension of *S*-acetyl acid **21** (200 mg, 0.578 mmol) and cesium carbonate (188 mg, 0.578 mmol) in 3 mL of DMF was added methyl iodide (0.5 mL, 1.16 mmol). The reaction mixture was stirred for 1 h, concentrated, and taken up in ethyl acetate. The organic layer was washed with water and brine, dried ($MgSO_4$), concentrated, and flash chromatographed on silica gel, eluting with ethyl acetate/hexanes (1:4) to give 68 mg (34%) of **22b** followed by 56 mg (28%) of **22a**.

22a (*S,S*): ^{1}H NMR ($CDCl_3$) δ 7.14 (m, 4H), 5.84 (d, 1H), 4.08 (q, 1H), 3.68 (s, 3H), 3.27 (d, 2H), 2.95 (m, 5H), 2.37 (s, 3H), 1.95 (q, 2H), 1.7−1.0 (6H).

22b (*R,S*): ^{1}H NMR ($CDCl_3$) δ 7.25 (m, 4H), 5.55 (d, 1H), 4.65 (m, 1H), 3.68 (s, 3H), 3.27 (d, 2H), 3.1 (m, 1H), 2.9 (m, 1H), 2.8 (d, 2H), 2.5 (m, 1H), 2.36 (s, 3H), 2.1 (m, 1H), 1.7−1.0 (m, 7H).

Methyl 2(*S*)-[(acetylthio)methyl]-2,3,4,5,6,7,8,9-octahydro-3-oxo-1*H*-4-benzazacycloundecine-5(*S*)-carboxylate (24a): ^{1}H NMR ($CDCl_3$) δ 7.1 (m, 4H), 5.61 (d, 1H), 3.9 (m, 1H), 3.62 (s, 3H), 3.1 (m, 2H), 2.9 (d, 1H), 2.6 (m, 2H), 2.45 (m, 1H), 2.3 (s, 3H), 2.1−1.0 (m, 7H).

Methyl 2(*R*)-[(acetylthio)methyl]-2,3,4,5,6,7,8,9-octahydro-3-oxo-1*H*-4-benzazacycloundecine-5(*S*)-carboxylate (24b): ^{1}H NMR ($CDCl_3$) δ 7.16 (m, 4H), 5.60 (d, 1H), 4.5 (m, 1H), 3.63 (s, 3H), 3.20 (d, 2H), 3.0 (m, 1H), 2.7 (m, 1H), 2.5 (m, 2H), 2.32 (s, 3H), 2.0 (m, 4H), 1.45 (m, 3H).

Methyl 2(*S*)-[(acetylthio)methyl]-2,3,4,5,6,7,8,9,10,11-decahydro-3-oxo-1*H*-4-benzazacyclotridecine-5(*S*)-carboxylate (26a): ^{1}H NMR ($CDCl_3$) δ 7.2 (m, 1H), 7.1 (m, 3H), 6.1 (d, 1H), 4.4 (m, 1H), 3.71 (s, 3H), 3.27 (d, 2H), 3.15 and 3.10 (dd, 2H), 2.85 (m, 1H), 2.55 (m, 2H), 2.37 (s, 3H), 1.75 (m, 1H), 1.5−1.1 (m, 9H); MS *m/e* 392 (M + 1).

Methyl 2(*R*)-[(acetylthio)methyl]-2,3,4,5,6,7,8,9,10,11-decahydro-3-oxo-1*H*-4-benzazacyclotridecine-5(*S*)-carboxylate (26b): ^{1}H NMR ($CDCl_3$) δ 7.3 (d, 1H), 7.2 (m, 1H), 7.1 (m, 2H), 5.86 (d, 1H), 4.63 (m, 1H), 3.70 (s, 3H), 3.2 (m, 3H), 2.7 (m, 3H), 2.4 (m, 1H), 2.31 (s, 3H), 1.9 (m, 1H), 1.5−1.2 (m, 9H).

Benzyl 2(*S*)-[(acetylthio)methyl]-2,3,4,5,6,7,8,9,10,11-decahydro-3-oxo-1*H*-4-benzazacyclotridecine-5(*S*)-carboxylate (44a): ^{1}H NMR ($CDCl_3$) δ 7.4 (m, 1H), 7.25 (m, 1H), 7.1 (m, 2H), 6.11 (d, 1H), 5.14 (AB q, 2H), 4.45 (m, 1H), 3.22 (d, 2H), 3.13 (m, 1H), 2.9 (m, 2H), 2.6 (m, 3H), 2.35 (s, 3H), 1.8 (m, 1H), 1.6−1.2 (m, 9H).

Benzyl 2(*R*)-[(acetylthio)methyl]-2,3,4,5,6,7,8,9,10,11-decahydro-3-oxo-1*H*-4-benzazacyclotridecine-5(*S*)-carboxylate (44b): ^{1}H NMR (DMSO-d_6) δ 7.3 (m, 5H), 7.15 (m, 4H), 5.88 (d, 1H), 5.1 (AB q, 2H), 4.69 (m, 1H), 3.2 (m, 3H), 2.65 (m, 2H), 2.3 (s, 3H), 2.4 (m, 1H), 1.9 (m, 1H), 1.6−1.0 (m, 10H); MS *m/e* 468 (M + 1). Anal. ($C_{27}H_{33}NO_4S$) C, H, N.

1,2,3,4,5,6,7,8,9,10-Decahydro-2(*S*)-mercapto-3-oxo-4-benzazacyclododecine-5(*S*)-carboxylic Acid (23a). To a deoxygenated solution of the *S*-acetyl ester **22a** (56 mg, 0.15 mmol) in 5 mL of THF and 1.5 mL of water was added 3 equiv of lithium hydroxide. The mixture was stirred 4 h at room temperature, concentrated, then taken up in a minimal amount of water, and acidified with 1 N HCl. The precipitate was collected and washed with a small amount of water and then hexanes to give 41 mg (84%) of **23a** melting at 222−225 °C: ^{1}H NMR (DMSO-d_6) δ 12.45 (br, 1H), 8.1 (d, 1H), 7.1 (m, 4H), 4.04 (m, 1H), 3.5−2.2 (m, 7H), 1.8−1.0 (m, 8H); MS *m/e* 322 (M + 1). Anal. ($C_{17}H_{23}NO_3S$) C, H, N.

1,2,3,4,5,6,7,8,9,10-Decahydro-2(*R*)-mercapto-3-oxo-4-benzazacyclododecine-5(*S*)-carboxylic Acid (23b): prepared similarly from **22b** was the thiol acid **23b** melting at 127−131 °C; ^{1}H NMR (DMSO-d_6) δ 12.4 (br, 1H), 8.04 (d, 1H), 7.2 (m, 4H), 4.42 (m, 1H), 3.0−2.0 (m, 7H), 1.8−1.0 (m, 8H): MS *m/e* 322 (M + 1). Anal. ($C_{17}H_{23}NO_3S$) C, H, N.

2,3,4,5,6,7,8,9-Octahydro-2(*S*)-mercapto-3-oxo-1*H*-4-benzazacycloundecine-5(*S*)-carboxylic Acid (25a): ^{1}H NMR (DMSO-d_6) δ 12.5 (s, 1H), 8.24 (d, 1H), 7.1 (m, 4H), 4.0 (t, 1H), 3.15 (t, 1H), 3.0−2.6 (m, 3H), 2.3 (m, 3H), 2.0 (m, 1H), 2.85 (m, 1H), 1.5 (m, 3H), 1.3 (m, 1H): MS *m/e* 308 (M + 1). Anal. ($C_{16}H_{21}NO_3S$) C, H, N.

2,3,4,5,6,7,8,9-Octahydro-2(*R*)-mercapto-3-oxo-1*H*-4-benzazacycloundecine-5(*S*)-carboxylic Acid (25b): ^{1}H NMR (DMSO-d_6) δ 12.7 (br, 1H), 7.85 (br, 1H), 7.14 (m, 4H), 4.3 (m, 1H), 3.07 (m, 1H), 2.9−2.5 (m, 3H), 2.3 (m, 3H), 2.0 (m, 1H), 2.8 (m, 1H), 1.4 (m, 3H), 1.25 (m, 1H); MS *m/e* 308 (M + 1). Anal. ($C_{16}H_{21}NO_3S$) C, H, N.

2,3,4,5,6,7,8,9,10,11-Decahydro-2(*S*)-mercapto-3-oxo-1*H*-4-benzazacyclotridecine-5(*S*)-carboxylic Acid (27a): $_1$H NMR (DMSO-d_6) δ 12.4 (br, 1H), 8.24 (d, 1H), 7.2 (m, 1H), 7.1 (m, 3H), 4.17 (m, 1H), 3.3−3.05 (m, 3H), 2.7 (m, 2H), 2.4 (m, 1H), 1.8−1.11 (m, 11H); MS *m/e* 336 (M + 1). Anal. ($C_{18}H_{25}NO_3S$) C, H, N.

2,3,4,5,6,7,8,9,10,11-Decahydro-2(*R*)-mercapto-3-oxo-1*H*-4-benzazacyclotridecine-5(*S*)-carboxylic Acid (27b): ^{1}H NMR (DMSO-d_6) δ 12.3 (br, 1H), 8.24 (m, 1H), 7.2 (m, 1H), 7.1 (m, 3H), 4.40 (m, 1H), 3.1 (d, 1H), 2.87 (m, 3H), 2.3 (m, 1H), 1.8 (m, 1H), 1.7−1.1 (m, 11H); MS *m/e* 336 (M + 1). Anal. ($C_{18}H_{25}NO_3S$) C, H, N.

4-[(2-Bromophenyl)methyl]-3-*t*-Boc-2,2-dimethyloxazolidine (28). To a solution of 2-N-Boc-3-(2-bromophenyl)-propanol (27.2 g, 82.4 mmol) in 200 mL of methylene chloride were added *p*-toluenesulfonic acid hydrate (1.56 g, 8.2 mmol) and 2,2-dimethoxypropane (100 mL). The solution was stirred at room temperature for 2 days. The reaction mixture was washed with $NaHCO_3$ and brine, dried over $MgSO_4$, filtered, and evaporated to dryness to give 30.1 g (98%) of **28** as an oil: ^{1}H NMR ($CDCl_3$) δ 7.55 (d, 1H), 7.23 (m, 2H), 7.07 (m, 1H), 4.23 (m, 1H), 3.7 (m, 2H), 3.2 (m, 1H), 2.9 (m, 1H), 1.7, 1.57 (two s, 6H), 1.45 and 1.40 (two s, 9H).

2-[(3-*t*-Boc-2,2-dimethyloxazolidinyl)methyl]benzaldehyde (29). The aryl bromide **28** (28.0 g, 75.6 mmol) in 1000 mL of THF was cooled to −78 °C. A solution of 2.5 N nBuLi (48 mL, 0.12 mol) was added dropwise. After completion of nBuLi addition, DMF (11 mL) was added, and the mixture was warmed to 0 °C over a 1 h period. The reaction solution was poured into ice water and extracted with ether two times. The ethereal layer was washed with water (2×) and brine (2×), dried over $MgSO_4$, filtered, and evaporated to

dryness. The residue was flash chromatographed on silica gel, eluting with ether/hexane (3:7), affording 18.5 g (87%) of **29**: ^{1}H NMR ($CDCl_3$) δ 10.45 and 10.35 (two s, 1H), 7.86 (d, 1H), 7.5 (q, 1H), 7.4 (q, 1H), 7.3 (q, 1H), 4.16 (m, 1H), 3.77 (m, 2H), 3.6−3.4 (m, 1H), 3.2 and 3.15 (2d, 1H), 1.7, 1.6, 1.55, 1.50 (four s, 6H), 1.4 and 1.35 (two s, 9H).

Ethyl 6-[2-[(3-*t*-Boc-2,2-dimethyloxazolidinyl)methyl]-phenyl]-5-hexenoate (30). To an ice bath cooled solution of aldehyde **29** (6.8 g, 21.3 mmol) and ethyl 5-triphenylphosphonium valerate iodide (22.1 g, 42.6 mmol) in 500 mL of methylene chloride was added 1.0 M potassium *tert*-butoxide in THF (42.6 mL, 42.6 mmol). The reaction mixture was allowed to warm to room temperature and stirred for 1 h. Silica gel (25 g) was added, and the mixture was concentrated, added to a silica gel column, and chromatographed, eluting with ethyl acetate/hexane (1:9), affording 7.4 g (80%) of **30**: ^{1}H NMR ($CDCl_3$) δ 7.18 (m, 4H), 6.63 (m, 1H), 5.7 (m, 1H), 4.08 (q, 2H), 4.05 (m, 1H), 3.68 (m, 2H), 3.1 (m, 1H), 2.7 (m, 1H), 2.4−2.1 (m, 4H), 1.72 (t, 2H), 1.68 (s, 3H), 1.54 (s, 3H), 1.47 (s, 3H), 1.2 (t, 3H).

6-[2-[(3-*t*-Boc-2,2-dimethyloxazolidinyl)methyl]phenyl]-5-hexenol (31). To an ice bath cooled solution of ester **30** (7.4 g, 17.2 mmol) was added lithium aluminum hydride (0.65 g, 17.2 mmol). The reaction mixture was stirred for 1 h and then quenched with water (0.6 mL), 15% NaOH (0.6 mL), and water (1.95 mL). To the mixture were added ethyl acetate (150 mL) and magnesium sulfate, and the mixture was stirred for 30 min. The solids were removed by filtration, and the filtrate was concentrated to give 6.9 g of **31**. The material was used as is in the next reaction: ^{1}H NMR ($CDCl_3$) δ 7.2 (m, 4H), 6.6 (m, 1H), 5.75 (m, 1H), 4.1 (m, 1H), 3.7 (m, 2H), 3.6 (m, 2H), 3.1 (m, 1H), 2.7 (t, 1H), 2.2 (q, 2H), 1.7−1.6 (m, 4H), 1.6−1.5 (br s, 6H), 1.5 (s, 9H).

6-[2-[(3-*t*-Boc-2,2-dimethyloxazolidinyl)methyl]phenyl]-5-hexenal (32). Pyridium chlorochromate (8.9 g, 35.4 mmol) was added to a solution of **31** (6.9 g, 17.7 mmol) in 100 mL of methylene chloride. The dark mixture was stirred for 30 min. The organic phase was decanted from the chromate salts. The solids were washed with ether, and the combined extracts were filter through a small pad of silica gel to give 6.3 g of **32.** The material was used as is in the next reaction: ^{1}H NMR ($CDCl_3$) δ 7.2 (m, 4H), 6.6 (m, 1H), 5.75 (m, 1H), 4.1 (m, 1H), 3.68 (m, 2H), 3.6 (m, 2H), 3.1 (m, 1H), 2.7 (t, 1H), 2.4 (t, 2H), 2.2 (q, 2H), 1.74 (t, 2H), 1.68 (s, 3H), 1.65 (br s, 3H), 1.5 (s, 9H).

6-[2-[(3-*t*-Boc-2,2-dimethyloxazolidinyl)methyl]phenyl]-5-hexenylidenepropanedioic Acid 1-Benzyl 3-Methyl Ester (33). A mixture of benzyl methyl malonate (3.56 g, 16.2 mmol), piperidine (207 mg, 2.4 mmol), benzoic acid (199 mg, 1.6 mmol), and the aldehyde **32** (6.3 g, 16.2 mmol) in 100 mL of toluene was refluxed with water removal using a Dean−Stark condenser for 6 h. The mixture was cooled to room temperature, stirred overnight, and diluted with ether. The organic layer was washed with 1 N HCl (2×), $NaHCO_3$ (2×), and brine (2×), dried ($MgSO_4$), and evaporated to dryness. The residue was chromatographed on silica gel, eluting with methylene chloride/ethylacetate (95:5) to give 4.3 g of **33** as a mixture of geometric isomers.

6-[2-[(3-*t*-Boc-2,2-dimethyloxazolidinyl)methyl]phenyl]-5-hexylpropanedioic Acid 1-Methyl Ester (34). A suspension of 10% Pd/C (3.0 g) and diester **33** (4.27 g, 7.4 mmol) in 150 mL of ethyl acetate was hydrogenated at 50 psi for 17 h. The reaction mixture was concentrated and filtered through a pad of celite. The solvent was removed to give 3.62 g of **34** used as is in the next step: ^{1}H NMR ($CDCl_3$) δ 7.2 (m,4H), 4.08 (m, 1H), 3.72 (s, 3H), 3.7 (m, 2H), 3.32 (t, 2H), 3.1 (m, 1H), 2.7 (m, 5H), 1.9 (m, 3H), 1.7−1.2 (m, 19H).

[6-[2-(2-Amino-3-hydroxypropyl)phenyl]hexyl]propanedioic Acid 1-Methyl Ester (35). A solution of **34** (3.62 g, 7.36 mmol) in 200 mL of methylene chloride at 0 °C was purged with dry HCl gas for 5 min. The ice bath was removed, HCl gas was bubbled into the solution for an additional 5 min, and the mixture was stirred at room temperature overnight. The solvent was removed, and the residue **35** (2.9 g) was used as is in the next step.

2,3,4,5,6,7,8,9,10,11-Decahydro-2-(hydroxymethyl)-4-oxo-1*H*-3-benzazacyclotridecine-5-carboxylic Acid (36). To a solution of EDCI (2.86 g, 14.9 mmol) and hydroxybenzotriazole (1.51 g, 11.2 mmol) in 3.3 L of methylene chloride was slowly added **35** (2.9 g, 7.47 mmol) in triethylamine (0.75 g, 7.4 mmol) and 450 mL of methylene chloride. The solution was mixed with a mechanical stirrer overnight. The solvent was removed under reduced pressure, and the residue was taken up in ethyl acetate and sodium bicarbonate. The organic layer was separated. The aqueous layer was reextracted with ethyl acetate, and the organics were combined, washed with 1 N HCl and brine, dried ($MgSO_4$), filtered, and evaporated to dryness. The residue was chromatographed on silica gel, eluting with ethyl acetate to give 1.46 g (59%) of **36** as a mixture of diastereomers after combining fractions: ^{1}H NMR ($CDCl_3$) δ 7.14 (m, 4H), 6.68 (d, 1H), 4.1 (m, 1H), 3.95−3.72 (m, 2H), 3.7 (s, 3H), 3.2 (m, 1H), 2.95 (d, 2H), 2.68 (t, 2H), 1.8−1.2 (m, 10H); MS *m*/*e* 334 (M + 1).

(±)-*cis*-Methyl 2-[(Acetylthio)methyl]-2,3,4,5,6,7,8,9,10,-11-decahydro-3-oxo-1*H*-4-benzazacyclotridecine-5-carboxylate (39a) and (±)-*trans*-Methyl 2-[(Acetylthio)-methyl]-2,3,4,5,6,7,8,9,10,11-decahydro-3-oxo-1*H*-4-benzazacyclotridecine-5-carboxylate (39b). To a suspension of *S*-acetyl acid (920 mg, 2.44 mmol) and cesium carbonate (794 mg, 2.44 mmol) in 7 mL of DMF was added methyl iodide (0.692, 4.87 mmol). The reaction mixture was stirred for 17 h, concentrated, and taken up in ethyl acetate. The organic layer was washed with water and brine, dried ($MgSO_4$), concentrated, and flash chromatographed on SiO_2, eluting with hexane/methylene chloride (1:1) and then ethyl acetate/methylene chloride (1:9) to give 188 mg of **39b** followed by 150 mg of **39a**.

39a: ^{1}H NMR ($CDCl_3$) δ 7.15 (m, 3H), 7.0 (m, 1H), 5.65 (d, 1H), 4.75 (m, 1H), 3.85 (s, 3H), 3.3 (t, 2H), 2.96 (d, 2H), 2.3 (m, 1H), 2.52 (m, 2H), 2.28 (s, 3H), 1.6−1.2 (m, 10H); MS *m*/*e* 392 (M + 1).

39b: 7.12 (m, 3H), 6.96 (d, 1H), 6.1 (d, 1H), 5.1 (m, 1H), 3.77 (s, 3H), 3.40 and 3.32 (dd, 1H), 3.15 and 3.10 (dd, 1H), 2.91 (d, 2H), 2.64 (t, 2H), 2.4 (m, 1H), 2.3 (s, 3H), 1.7−1.2 (m, 10H); MS *m*/*e* 392 (M + 1).

(±)-*trans*-Methyl 2-[(acetylthio)methyl]-1,2,3,4,5,6,7,8,9,-10-decahydro-3-oxo-4-benzazacyclododecine-5-carboxylate (37b): ^{1}H NMR ($CDCl_3$) δ 7.2 (m, 2H), 7.1 (t, 1H), 6.9 (d, 1H), 5.81 (d, 1H), 5.18 (m, 1H), 3.8 (s, 3H), 3.45 and 3.40 (dd, 1H), 3.17 and 3.10 (dd, 1H), 2.91 (d, 2H), 2.80 (m, 1H), 2.36 (m, 2H), 2.28 (s, 3H), 1.9−1.1 (m, 8H).

(±)-*cis*-Methyl 2-[(acetylthio)methyl]-1,2,3,4,5,6,7,8,9,-10,11,12-dodecahydro-3-oxo-4-benzazacyclotetradecine-5-carboxylate (41a): ^{1}H NMR ($CDCl_3$) δ 7.17 (m, 4H), 5.88 (d, 1H), 4.50 (m, 1H), 3.78 (s, 3H), 3.2 (m, 2H), 3.08 and 3.0 (dd, 1H), 2.9 and 2.86 (dd, 1H), 2.7 (m, 1H), 2.5 (m, 1H), 2.3 (m, 1H), 2.25 (s, 3H), 1.6−1.2 (m, 12H); MS *m*/*e* 406 (M + 1).

(±)-*trans*-Methyl 2-[(acetylthio)methyl]-1,2,3,4,5,6,7,8,9,-10,11,12-decahydro-3-oxo-4-benzazacyclotetradecine-5-carboxylate (41b): ^{1}H NMR ($CDCl_3$) δ 7.l4 (m, 4H), 5.9 (d, 1H), 5.22 (m, 1H), 3.84 (s, 3H), 3.1 (m, 2H), 2.9 (d, 2H), 2.64 (m, 1H), 2.48 (m, 1H), 2.3 (m, 1H), 2.28 (s, 3H), 1.7 (m, 1H), 1.6−1.2 (m, 11H); MS *m*/*e* 406 (M + 1).

(±)-*cis*-2,3,4,5,6,7,8,9,10,11-Decahydro-2-mercapto-3-oxo-1*H*-4-benzazacyclotridecine-5-carboxylic Acid (40a). To a deoxygenated solution of the *S*-acetyl ester **39a** (135 mg, 0.34 mmol) in 5 mL of THF, 1 mL of water, and 1 mL of methanol was added 3 equiv of lithium hydroxide. The mixture was stirred for 4 h at room temperature, concentrated, taken up in a minimal amount of water, and acidified with 1 N HCl. The precipitate was collected and washed with a small amount of water and then hexanes to give 109 mg (95%) of **40a**[21] melting at 178−182 °C: ^{1}H NMR (DMSO-d_6) δ 12.3 (br, 1H), 8.6 and 8.55 (two d, 1H), 7.25 (m, 1H), 7.1 (m, 3H), 3.92 (m, 1H), 3.2 (m, 2H), 2.7 (m, 1H), 2.6 (m, 2H), 2.35 (m, 2H), 2.2 (m, 1H), 1.6−1.0 (m, 10H); MS *m*/*e* 336 (M + 1). Anal. ($C_{18}H_{25}NO_3S$) C, H, N.

(±)-*trans*-2,3,4,5,6,7,8,9,10,11-Decahydro-2-mercapto-3-oxo-1*H*-4-benzazacyclotridecine-5-carboxylic Acid (40b): prepared similarly from **39b** was the thiol acid **40b**[21] melting at 179−183 °C; ^{1}H NMR (DMSO-d_6) δ 12.8 (br, 1H), 8.6 and 8.55 (two d, 1H), 7.25 (m, 4H), 4.4 (m, 1H), 3.1 (m, 2H), 2.8 (m, 2H), 2.6 (m, 2H), 2.4−2.1 (m, 2H), 1.6−1.0 (m, 10H); MS *m*/*e* 336 (M + 1). Anal. ($C_{18}H_{25}NO_3S$) C, H, N.

(±)-*trans*-1,2,3,4,5,6,7,8,9,10-Decahydro-2-mercapto-3-oxo-4-benzazacyclododecine-5-carboxylic Acid (38b): ^{1}H NMR (DMSO-d_6) δ 12.5 (br, 1H), 8.24 (d, 1H), 7.2 (m, 2H), 7.1 (m, 2H), 4.80 (m, 1H), 3.08 (d, 2H), 2.62 (m, 2H), 2.3 (t, 1H), 2.0 (m, 2H), 1.9−1.5 (m, 2H), 1.3 (m, 4H), 1.0 (m, 2H): Anal. ($C_{17}H_{23}NO_3S$) C, H, N.

(±)-*cis*-1,2,3,4,5,6,7,8,9,10,11,12-Dodecahydro-2-mercapto-3-oxo-4-benzazacyclotetradecine-5-carboxylic Acid (42a): ^{1}H NMR (DMSO-d_6) δ 12.4 (br, 1H), 8.55 and 8.52 (two d, 1H), 7.23 (m, 1H), 7.1 (m, 3H), 4.06 (m, 1H), 3.2 (m, 1H), 3.05 (m, 1H), 2.96 (m, 1H), 2.61 (m, 2H), 2.4 (m, 3H), 1.8−1.0 (m, 12H); MS *m*/*e* 350 (M + 1). Anal. ($C_{19}H_{27}NO_3S$) C, H, N.

(±)-*trans*-1,2,3,4,5,6,7,8,9,10,11,12-Dodecahydro-2-mercapto-3-oxo-4-benzazacyclotetradecine-5-carboxylic Acid (42b): ^{1}H NMR (DMSO-d_6) δ 12.6 (br, 1H), 8.48 (d, 1H), 7.2 (m, 1H), 7.1 (m, 3H), 4.7 (m, 1H), 3.0 (m, 2H), 2.8 (m, 1H), 2.65 (m, 3H), 2.4 (m, 1H), 1.8−1.0 (m, 12H); MS *m*/*e* 350 (M + 1).

Modeling of Compounds in Thermolysin. A model of the binding site of thermolysin was constructed using the crystal structure of Cbz-Gly^P-Leu-Leu ("Gly^P" = $NHCH_2PO_2-$) bound with thermolysin.[15] The structure, labeled 5TMN, was obtained from the Brookhaven Protein Data Bank.[16,17] Only those binding site residues which are near the inhibitors were included in the calculation. The following residues were included: Asn 111, Asn 112, Ala 113, Phe 114, Trp 115, Asn 116, Gly 118, Ser 118, Gly 119, Met 120, Val 121, Tyr 122, Gly 123, Phe 130, Leu 133, Asp 138, Val 139, Val 140, Ala 141, His 142, His 143, His 146, Tyr 157, Ser 169, Asp 180, Glu 165, Glu 166, Ile 188, Gly 189, Gly 190, Val 192, Tyr 193, Leu 202, Arg 203, Asp 226, Val 227, Val 230, His 231, and Val 232.

The X-ray models of different thermolysin/inhibitor complexes show small changes in the conformation of a few residues. In our computer model, residues with the largest amounts of variability (Glu 143) was allowed to move freely during the energy minimization step. Residues found near the inhibitor that show smaller amounts of movement (Asn 112, Leu 133, Val 139, and Leu 202) were constrained with a small force constant of 0.5 kJ. The remaining residues which form a shell around the more flexible residues were constrained with a force constant of 500.0 kJ.

To determine if a molecule can fit into the active site of thermolysin, each molecule was constructed using the interactive molecular modeling program, MACROMODEL.[18] To construct the various macrocycles, the conformation of thiorphan from the thiorphan/thermolysin crystal structure served as a starting point. The sulfur atom was bound to the zinc with a zero-order bond. The structure was then energy minimized using the AMBER force field[19] as implemented by the QXP program.[14] The Monte Carlo/energy minimization protocol of the MCDOCK module of the QXP program was used with 1000 search and energy minimization cycles resulting in a thorough conformational search assuring the exploration of a variety of different binding modes. Previous work using the BATCHMIN[18] program of MACROMODEL describes the binding site model and gives the parameters used for the zinc−sulfur geometry.[20]

After energy minimization within the active site, a conformational search was conducted to determine the lowest energy conformation of the molecule in the absence of the enzyme. The difference between the energy of the bound conformation and the energy of the conformation minimized outside the binding sites was taken as a measure of the ligand strain energy. A ligand strain energy above 25 kJ is taken to be excessively high, indicating that the bound conformation is not energetically accessible to that molecule.

The total energy between the ligand and the binding site atoms is also reported. This energy is defined as the sum of the interaction energy, the enzyme strain energy, and ligand strain energies.[14] This energy has been found to be a useful qualitative guide to distinguish between the ligands that form good interactions with the binding site and those that cannot.

The final steps of the evaluation of a docked structure is visual. After conformational searching and energy minimization in the binding site, the structures are scrutinized to determine if they can form the hydrogen bonds and hydrophobic interactions known to occur in the thermolysin/inhibitor crystal structures of similar inhibitors.

Acknowledgment. We thank the CIBA analytical staff in Summit, NJ, for collecting the analytical data. We also thank Ms. C. Berry and Ms.Y. Sakane for assistance in *in vitro* measurements of NEP, TLN, and ACE. The QXP modeling program software is available from Colin McMartin.

References

(1) Winquist, R. J.; Hintze, T. H. Mechanisms of Atrial Natriuretic Factor-Induced Vasodilation. *Pharmacol. Ther.* **1990**, *48*, 417−426. (b)Ruskoaho, H. Atrial Natriuretic Peptide: Synthesis, Release, and Metabolism. *Pharmacol. Rev.* **1992**, *44*, 479−602.

(2) Tonolo, G.; Richards, A. M.; Manunta, P.; Pazzola, A.; Madeddu, P.; Towrie, R.; Fraser, R.; Glorioso, N. Low-Dose Infusion of Atrial Natriuretic Factor in Mild Essential Hypertension. *Circulation* **1989**, *80*, 893−902 and references cited therein.

(3) (a) McMartin, C.; Hagen, M. E.; Sytwu, I.; Webb, R. L.; Wennogle, L. P.; Zimmerman, M. B. Degradation of Atrial Natriuretic Peptide (ANP): Effects of Endopeptidase EC. 24.11 Inhibition on Catabolism. *FASEB J.* **1988**, *2*, A936. (b) Wennogle, L. P.; Ghai, R.; McMartin, C.; Webb, R. L.; Erion, M.; Gilligan, J.; Oei, H.; Zimmerman, M. B. Multiple Mechanisms Mediate Disappearance of ANF from the Vascular Compartment in the Rat. In *Biol. Mol. Aspects Atrial Factors* **1988**, 13−27. (c) Zimmerman, M. B.; McMartin, C. M.; Yasay, G.; Wennogle, L. P.; Webb, R. L. Degradation of Atrial Natriuretic Peptide: Pharmacologic Effects of Protease EC 24.11 Inhibition. *FASEB J.* **1988**, *2*, A937. (d) Trapani, A. J.; Smits, G. J.; McGraw, D. E.; Spear, K. L.; Koepke, J. P.; Olins, G. M.; Blaine, E. H. Thiorphan, an Inhibitor of Endopeptidase 24.11, Potentiates the Natriuretic Activity of Atrial Natriuretic Peptide. *J. Cardiovasc. Pharmacol.* **1989**, *14*, 419−424. (e) Webb, R. L.; Yasay, G. D.; McMartin, C.; McNeal, R. B.; Zimmerman, M. B. Degradation of Atrial Natriuretic Peptide: Pharmacologic Effects of Protease EC 24.11 Inhibition. *J. Cardiovasc. Pharmacol.* **1989**, *14*, 285−293 (f) Gros, C.; Souque, A.; Schwartz, J.-C. Inactivation of Atrial Natriuretic Factor in Mice in Vivo: Crucial Role of Enkephalinase (EC 3.4.24.11). *Eur. J. Pharmacol.* **1990**, *179*, 45−56. (g) Toll, L.; Brandt, S. R.; Olsen, C. M.; Judd, A. K.; Almquist, R. G. Isolation and Characterization of a New Atrial Peptide-Degrading Enzyme from Bovine Kidney. *Biochem. Biophys. Res. Commun.* **1991**, *175*, 886−893. (h) Vanneste, Y.; Pauwels, S.; Lambotte, L.; Michel, A.; Dimaline, R.; Deschodt-Lanckman, M. Respective Roles of Kallikrein and Endopeptidase 24.11 in the Metabolic Pathway of Atrial Natriuretic Peptide in the Rat. *Biochem. J.* **1990**, *269*, 801−806.

(4) Roques, B. P.; Noble, F.; Daugé, V.; Fournier-Zaluski, M.-C.; Beaumont, A. Neutral Endopeptidase 24.11: Structure, Inhibition, and Experimental and Clinical Pharmacology. *Pharmacol. Rev.* **1993**, *45*, 87−146.

(5) (a) Danilewicz, J. C.; Barclay, P. L.; Barnish, I. T.; Brown, S. F.; Campbell, S. F.; James, K.; Samuels, G. M. R.; Terrett, N. K.; Wythes, M. J. UK-69,578, a Novel Inhibitor of EC 3.4.24.11 which Increases Endogenous ANF Levels and Is Natriuretic and Diuretic. *Biochem. Biophys. Res. Commun.* **1989**, *164*, 58−65. (b) Erdos, E. G.; Skidgel, R. A. Neutral Endopeptidase 24.11 (Enkephalinase) and Regulators of Peptide Hormones. *FASEB J.* **1989**, *3*, 145−151. (c) Gros, C.; Souque, A.; Schwartz, J.-C.; Duchier, J.; Cournot, A.; Baumer, P.; Lecomte, J.-M. Protection of Atrial Natriuretic Factor Against Degradation, Diuretic and Natriuretic Responses after Inhibition of Enkephalinase (EC 3.4.24.11). *Proc. Natl. Acad. Sci. U.S.A.* **1989**, *86*, 7580−7585. (d) Haslanger, M. F.; Sybertz, E. J.; Neustadt, B. R.; Smith, E. M.; Nechuta, T. L.; Berger, J. Carboxyalkyl Dipeptides with Atrial Natriuretic Factor Potentiating and Antihypertensive Activity. *J. Med. Chem.* **1989**, *32*, 739−742. (e) Sybertz, E. J.; Chiu, P. J. S.; Watkins, R. W.; Vemulapalli, S. Neutral Endopeptidase Inhibition: A Novel Means of Circulatory Modulation. *J. Hypertension* **1990**, *8* (suppl. 7), S161−S167. (f) Seymour, A. A.; Norman, J. A.; Asaad, M. M.; Fennell, S. A.; Swerdel, J. N.; Little, D. K.; Dorso, C. R. Renal and Depressor Effects of SQ 29,072, a Neutral Endopeptidase Inhibitor, in Conscious Hypertensive Rats. *J. Cardiovasc. Pharmacol.* **1990**, *16*, 163−172. (g) Seymour, A. A.; Norman, J. A.; Asaad, M. M.; Fennell, S. A.; Little, D. K.; Kratunis, V. J.; Rogers, W. L. Antihypertensive and Renal Activity of SQ 28,603, an Inhibitor of Neutral Endopeptidase. *J. Cardiovasc. Pharmacol.* **1991**, *17*, 296−304.

(6) MacPherson, L. J.; Bayburt, E. K.; Capparelli, M. P.; Bohacek, R. S.; Clarke, F. H.; Ghai, R. D.; Sakane, Y.; Berry, C. J.; Peppard, J. V.; Trapani, A. J. Design and Synthesis of an Orally Active Macrocyclic Netural Endopeptidase 24.11 Inhibitor. *J. Med. Chem.* **1993**, *36*, 3821−3828.

(7) Stanton, J. L.; Sperbeck, D. M.; Trapani, A. J.; Cote, D.; Sakane, Y.; Berry, C. J.; Ghai, R. D. Heterocyclic lactam derivatives as dual angiotensin coverting enzyme and neutral endopeptidase 24.11 inhibitors. *J. Med. Chem.* **1993**, 36, 3829−3833.

(8) Matthews, B. W. Structural Basis of the Action of Thermolysin and Related Zinc Peptidases. *Acc. Chem. Res.* **1988**, *21*, 333−340.
(9) Holland, D. R.; Karclay, P. L.; Danilewicz, J. C.; Matthews, B. W.; James, K. Inhibition of Thermolysin and Neutral Endopeptidase 24.11 by a Novel Glutaramide Derivative: X-ray Structure Determination of the Thermolysin-Inhibitor Complex. *Biochemistry* **1994**, *33*, 51−60.
(10) Benchetrit, T.; Fournié-Zaluski, M. C.; Roques, B. P. Relationship Between the Inhibitory Potencies of Thiorphan and Retrothiorphan Enantiomers on Thermolysin and Neutral Endopeptidase 24.11 and their Interactions with the Thermolysin Acitve Site by Computer Modeling. *Biochem. Biophys. Res. Commun.* **1987**, *147*, 1034−1040.
(11) Roques, B. P.; Lucas-Soroca, E.; Chaillet, P.; Costentin, J.; Fournié-Zaluski, M. Complete Differentiation Between Enkephalinase and Angiotensin-Converting Enzyme Inhibition by *Retro*-Thiorphan. *Proc. Natl. Acad. Sci. U.S.A.* **1983**, *80*, 3178−3182.
(12) Bohacek, R. S.; Priestle, J.; Grutter, M. Unpublished results.
(13) De Lombaert, S.; Erion, M. D.; Tan, J.; Blanchard, L.; El-Chehabi, L.; Ghai, R.; Sakane, Y.; Berry, C.; Trapani, A. J. N-Phosphonomethyl Dipeptides and Their Phophonate Prodrugs, a New Generation of Netural Endopeptidase (NEP, EC 3.4.24.11) Inhibitors. *J. Med. Chem.* **1994**, *37*, 498−511.
(14) McMartin, C.; Bohacek, R. QXP; a basic set of powerful, user friendly computer routines for structue-based drug design. *J. Comput.-Aided Mol. Des.*, in press.
(15) Holden, H. M.; Tronrud, D. E.; Monzingo, A. F.; Weaver, L. H.; Matthews, B. W. Slow- and Fast-Binding Inhibitors of Thermolysin Display Different Modes of Binding: Crystallographic Analysis of Extended Phosphonamidate Transition-State Analogues. *Biochemistry* **1987**, *26*, 8542−8553.
(16) Bernstein, F. C.; Koetzle, T. F.; Williams, G. J. B.; Meyer, E. F.; Brice, M. D.; Rodgers, J. R.; Kennard, T.; Shinamoucchi, T.; Tasumi, M. The Protein Data Bank: A Computer Based Archival File for Macromolecular Structures. *J. Mol. Biol.* **1977,** *112*, 535−542.
(17) Abol, E. E.; Bernstein, F. C.; Bryant, S. H.; Koetzle, T. F.; Weng, J. In *Crystallographic Databases-Information Content, Software Systems, Scientific Applications*; Allen, F. H., Bergerhoff, G., Sievers, R., Eds.; Data Commission of the International Union of Crystallography: Bonn/Cambridge/Chester, 1987; pp 107−132.
(18) Mohamadi, F.; Richards, N. G. J.; Guida, W. C.; Liskamp, R.; Lipton, M.; G., C.; Chang, G.; Hendirckson, T.; Still, W. C. MACROMODEL - An Integrated Software System for Modelling Organic and Bioorganic Molecules Using Molecular Mechanics. *J. Comput. Chem.* **1990**, *11*, 440−467.
(19) Weiner, S. J.; Kollman, P. A.; Case, D. A.; Singh, U. C.; Ghio, C.; Alagona, G.; Profeta, S.; Weiner, P. K. A New Force Field for Molecular Mechanical Simulation of Nucleic Acids and Proteins. *J. Am. Chem. Soc.* **1984**, *106*, 765−784.
(20) Guida, W. C.; Bohacek, R. S.; Erion, M. D. Probing the Conformational Space Available to Inhibitors in the Thermolysin Active Site Using Monte Carlo/Energy Minimization Techniques. *J. Comput. Chem.* **1992,** *13*, 214−228.
(21) Sample appears to be contaminated with 20−25% of the S−S dimer based on the ^{1}H NMR and the results obtained from an Ellmann SH test.
(22) The crystal structure of thiorphan bound to thermolysin has been reported.[8] However, because only the coordinates of thiorphan without those of thermolysin were released, Figure 2 shows thiorphan minimized in our thermolysin model. This conformation is almost identical to that from the crystal structure. The crystal structure of a close analog of the 10-membered macrocycle bound to thermolysin has also been determined (private communication, M. Gruetter). This structure agrees closely with our model of the 10-membered macrocycle shown in Figure 3.

JM960582O